On the correlation between morphology and Amplified Spontaneous Emission properties of a polymer:polymer blend.

Sandro Lattante[a,*], Arianna Cret´ı[b], Mauro Lomascolo[b], Marco Anni[a]

[a]Dipartimento di Matematica e Fisica ”Ennio De Giorgi”, Universit´a del Salento, via per Arnesano 73100 Lecce - Italy
[b]IMM-CNR Institute for Microelectronic and Microsystems, Via per Monteroni, 73100 Lecce, Italy

Abstract

We investigate the amplified spontaneous emission (ASE) properties of a prototypical host-guest polymer polymer blend, namely poly(9,9-dioctylfluorene) (PF8) and poly(9,9-dioctylfluorene-co-benzothiadiazole) (F8BT) blend, with different concentration ratio. We show that the initial F8BT content increase causes an increase of the F8BT ASE threshold, even leading to ASE suppression for F8BT contents between 25% and 75%. ASE is then recovered upon further increase of the F8BT relative content. We demonstrate that the ASE properties of the PF8:F8BT are dominated by morphology effects, like submicrometric phase segregation, determining the net gain of the active waveguides.

Keywords: Amplified Spontaneous Emission, Polymer Blends, Morphology, Confocal Laser Scanning Microscopy, FRET

_____

*Corresponding author: sandro.lattante@unisalento.it

1. Introduction

Since the discovery of electrical conductivity in conjugated polymers [1], the research efforts to develop high performing organic-based optoelectronic devices have been substantial, leading, to date, to full commercialization of various kind of organic optoelectronic devices [2]. With the aim to realize optimal polymeric systems for optoelectronic applications, two general routes are followed. The first is the development of novel polymeric molecules with tailored chemical and electronic properties. The second is to blend two or more known compounds in order to obtain new composites with properties different from the ones typical of each single components [3].

Among the various luminescent systems, the polymer-polymer blends are thus of particular importance due to the easy tuneability of the optical and electronic properties of the single components, and in view of possible optoelectronic applications involving bio-polymers [4, 5, 6, 7]. Generally speaking, when dealing with organic-based optoelectronic devices, the morphology of the organic layers has been identified as one of the primary parameter to be optimized in order to attain the highest performance [8]. This has been well established in organic solar cells [9], organic light emitting diodes [10] and organic field effect transistor [11, 12].

Morphological properties have been also demonstrated to be at the origin of some interesting lasing effects from organic thin films [13]. In this particular field, among the various active material for lasing action, conjugated polymers and oligomers have attracted lot of interest due to: 1) high optical gain; 2) easy processability of the devices starting from solutions in common organic solvents, using scalable and low cost fabrication process

such ink-jet printing, roll-to-roll printing, spin-coating; 3) easy tuneability of their emission properties simply by changing the nature and/or the position of the substituent groups attached to the core polymer chains [14, 15]. In particular the high optical gain - that has been demonstrated in several polymeric and oligomeric thin films [16, 17, 18, 19, 20] - can be conveniently exploited in many application like optical data communications [21], gas sensing [22, 23], organic lasers [24]. Although, to date, no electrically driven organic laser has been demonstrated [25], elegant and alternative device structures have been suggested to fully exploit the properties of organic lasing materials in an electrically controlled device [26]. The very first step in the development of novel lasing systems is the characterization of the optical gain of the active material.

Optical gain in thin films of polymers is evidenced by a strong line narrowing of the emission spectrum for excitation densities above a threshold value. The origin of the line narrowing has been typically attributed to Amplified Spontaneous Emission (ASE) supported by wave-guiding inside the film [27, 28, 29]. Since the ASE threshold decreases as the material optical gain increases (*ceteris paribus*), the ASE threshold minimization is a useful way to develop good materials for lasers. In the last years it has been demonstrated that the ASE threshold can be decreased by blending two different species, specifically selected in order to exploit the processes of energy transfer (in particular the Förster Resonant Energy Transfer - FRET) from the excited donor material to the acceptor material with optical gain [30, 31]. A necessary prerequisite for energy transfer to occur is the good overlap between the emission band of the donor and the absorption band of the acceptor.

As FRET can be very efficient also for small acceptor content in the blend, active blends typically show low ASE threshold due to the combination of high pump laser absorption from the donor, effective acceptor excitation by FRET and low losses due to self absorption and aggregation [32].

To date, the role of donor-to-acceptor concentration has been the subject of few studies focused on ASE from polymer:polymer blends exploiting FRET [30, 33]. In particular an improvement of the acceptor ASE with the acceptor content increase, followed by a saturation, has been observed [33], ascribed to a progressive FRET efficiency increase. More recently [34] it has been observed that the eventual acceptor aggregation decreases the ASE effect, dominating over the FRET increase at high enough acceptor content, thus determining the existence of an optimal concentration minimizing the acceptor ASE threshold. Anyway, it is well known that the major part of polymer blends undergo microscopic phase separation that locally changes the FRET efficiency [35] and that can likely add optical loss channels inside the film waveguide, thus potentially affecting the ASE process. Despite this observation, a clear correlation between donor-to-acceptor ratio, blend morphology and ASE is still lacking.

In this paper we investigate the ASE properties of poly(9,9-dioctylfluorene) (PF8):poly(9,9-dioctylfluorene-co-benzothiadiazole) (F8BT) blends [36] with different concentration ratios, chosen as prototypical host:guest polymer:polymer blend [37]. The PF8 photoluminescence (PL) [38] overlap with the F8BT absorption spectrum, thus fulfilling the necessary prerequisite for a good FRET to occur. We have correlated the optical gain properties of the blends with the blends morphology by Laser Scanning Microscopy. We show that the concentration ratio and the energy transfer process alone can not fully

describe the ASE behavior of the blends as previously reported [33]. We show that the PF8:F8BT phase segregation between the species has a deep impact on the ASE properties even in blends whose concentration ratio should be optimal from an energetic point of view, where we find a total suppression of any ASE effect. These results can be generalized to several polymer blend systems due to the generic phase segregation behavior of such systems, extending our results in contiguous fields like high performance organic-base LEDs and Light Emitting FETs.

2. Experimental

Individual PF8 and F8BT toluene solutions (15 mg/ml each) have been prepared and stirred overnight. PF8 solutions have been initially heated at about 70 °C for 5 minutes during stirring in order to avoid the formation of the PF8 beta phase [39] in the final samples. The F8BT relative content in the blend has been varied from 5% to 100% by mixing the appropriate content of the initial single solutions using LLG micro-pipettes. Eight samples with different F8BT relative contents have been investigated, named X-F8BT (where the X value indicates the F8BT percentage in the blend). The films have been prepared by spin coating the solutions on toluene-cleaned ultrathin microscopy cover glass slides (from Bresser, certified thickness of 130 170 μm) in air and at room temperature. The film thicknesses have been measured by a Dektat Alpha Step Profilometer; the obtained thickness values are reported in Tab. S1 in the Supporting Information. All the measured thicknesses are above the waveguide cut-off.
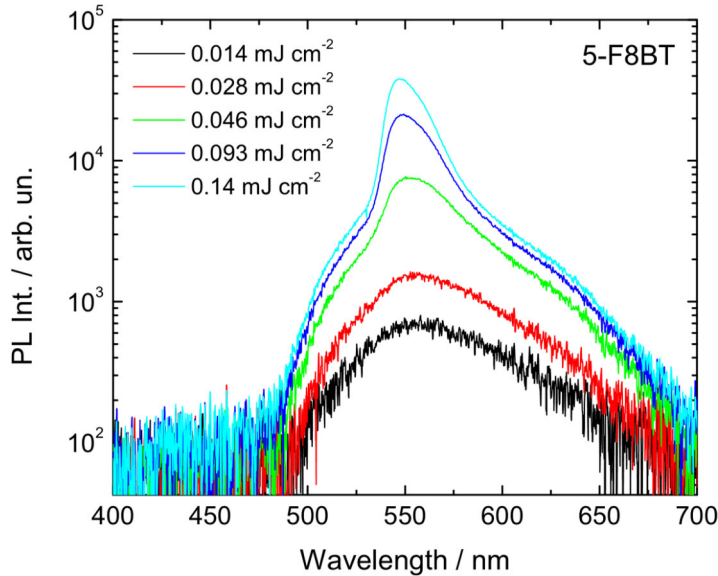
Figure 1: Sample 5-F8BT photoluminescence spectra as a function of the excitation density.

Room temperature Time-Resolved Photo-Luminescence (TR-PL) has been excited by the 400 nm line delivered by a solid state pulsed laser (mod. PLP10, Hamamatsu), which provides a pulse of about 58 ps at repetition rate of 1 MHz. The max peak power was of about 70 mW. The PL has been dispersed by an iHR320 (focal length of 0.32 m) Horiba monochromator equipped with a Peltier cooled Hamamatsu (Head-on mod R943-02), operating in single photon counting. The spectral resolution was about 4.8 nm for TR-PL experiments. Time-Correlated Single Photon Counting (TCSPC) technique has been used to record TR-PL in the spectral visible range by using an Edinburg Instruments TCC900 TSCPC electronics card.

ASE has been measured in a different experimental set-up, exciting the samples with the 337 nm emission from a Nitrogen laser, delivering 3 ns pulses with a repetition rate of 10 Hz. The excitation beam has been focused on the sample by a cylindrical lens, thus obtaining a rectangular excitation stripe with

width of about 100 μm and variable length up to 6 mm. Only the central region of the pump beam has been selected with a variable slit thus obtaining an homogeneous excitation density. The sample emission has been collected from the sample edge using an optical fiber connected to a SM442 Preconfigured CCD spectrometer. The spectral resolution was about 0.6 nm. ASE measurements have been performed at room temperature in a vacuum chamber (about 10^{-3} mbar) in order to avoid photo-oxidation at high excitation densities. The samples have been morphologically characterized by Confocal Laser Scanning Microscopy with a Nikon Eclipse C1 inverted confocal microscope using a 60X DIC Plan Apochromat oil-immersed objective (N.A. 1.4). The samples have been excited by both the 405 nm line of a diode laser and the 488 nm line of an argon laser, and the PL signal has been detected by a couple of photo-multipliers (PMTs). The signal was detected simultaneously at 450 ± 20nm and at 605 ± 30nm using bandpass filters, in order to map the PL of PF8 and F8BT, respectively.

3. Results and Discussion

The absorption spectra and the photoluminescence spectra of all of the samples are reported in Fig. S1 and in Fig. S2 in the S. I. The absorption main peaks of both the species are evident in the blends, while the PL is clearly dominated by the F8BT emission, suggesting efficient FRET in the blends.

Concentration dependence of the Amplified Spontaneous Emission. Fig. 1 reports the first 5 photoluminescence spectra as a function of the excitation density from the 5-F8BT sample in a semi-log scale. For excitation densities lower than 0.028 mJ cm^{-2} the spectra resembles the traditional

7

photoluminescence from the acceptor F8BT. As the excitation density increases over 0.040 mJ cm^{-2} a clear line narrowing peaked at about 540 nm appears, attributed to waveguide assisted ASE [29]. The FRET mechanism between the PF8 donor to the F8BT acceptor is clearly evident even for such a low acceptor content in the blend. Indeed the emission is almost completely from the F8BT phase (a low residual PF8 emission is detected peaked around 435 nm, see Fig. S2 in the Supporting Information, that is a signature of a non complete FRET from the donor phase to the acceptor phase [33]).

In order to determine the ASE threshold, we have considered the spectrum Full Width at Half Maximum (FWHM): ASE threshold has been determined as the excitation density at which the FWHM equals the average between the low excitation density value and the high excitation density value. The 5-F8BT ASE threshold thus results to be 0.26 mJ cm^{-2}.

When the F8BT content in the blend is further increased, we observe that (see Fig. 2):

- the ASE threshold increases to 0.39 mJ cm^{-2} in the 10-F8BT sample;

- no ASE is observed in the 25-F8BT, in the 50-F8BT and in the 75F8BT samples up to about 15 mJ cm^{-2};

- ASE is recovered in the 90-F8BT sample, with a very low threshold of 0.20 mJ cm^{-2} (the lowest of all the samples);
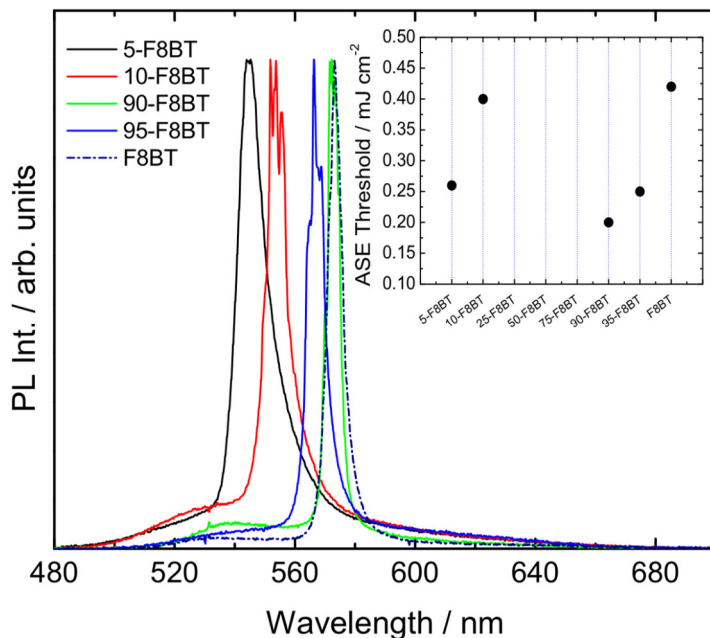
Figure 2: Spectral line narrowing of the PL emission from the X-F8BT samples.

- a further ASE threshold increase in the 95-F8BT sample to 0.25 mJ cm^{-2} and in the pure F8BT to 0.40 mJ cm^{-2}.

- a progressive red-shift of the ASE band, recorded between 540 and 570 nm. The peaks present in the ASE band of the 10-F8BT and of the 95-F8BT samples are due to random lasing effect [13, 40, 41].

The observed ASE threshold dependence on the F8BT content is clearly not consistent with the interplay between the PF8:F8BT FRET increase and the F8BT aggregation increase: in fact it is expected that the FRET efficiency should increase with increasing the acceptor content in the blend [33]: an initial decrease of the ASE threshold is typically evident with increasing acceptor content in the blend, up to a minimum for the optimum donor-toacceptor ratio, followed by an increasing threshold once the acceptor

9

content is further increased [34]. We on the contrary do not observe, as reported, a similar behavior.

Moreover it is possible to roughly estimate the FRET efficiency variation among the samples by determining the percentage of the PF8 emission over the total PL emission from the PL spectra for all the samples (see Fig. S2 in the S. I.). In particular we have found that in the 50-F8BT sample the PF8 residual emission accounts for only the 0.7% of the total PL emission, as well in the 25-F8BT accounts for only the 2.8%, thus the energy transfer mechanism (*via* FRET or other possible routes) should be very efficient [42]: anyway no ASE is observed in these samples.

Wave-guiding properties. In order to determine the origin of this unexpected ASE threshold behavior, we started from the investigation of the waveguiding properties of the active layer. In particular it has been recently demonstrated [43] that the ASE threshold decreases as the guided Mode Confinement (MC) increases and as the Pump to Mode Overlap increases (PMO), being inversely proportional to MC*PMO. Both MC and PMO have been calculated for all the investigated samples starting from the TE0 calculation, using the experimental thickness and as refractive index of the particular blend the relative concentration weighted average of the PF8 and F8BT refractive indexes at 540 nm (1.7 and 2 respectively, as extracted from [44]. The so calculated effective refractive indexes are reported in Tab. S1 in the S. I.). The obtained trend of ASE threshold is reported in Fig. 3. With the only exception of the threshold increase from sample 5-F8BT to 10-F8BT no agreement with the experimental thresholds is observed. In particular samples 25-F8BT, 50-F8BT and 75-F8BT should show a lower ASE threshold than 10-F8BT, while no ASE is observed. Moreover sample 90-F8BT should

show the highest ASE threshold, while it show the lowest, and the threshold should decrease in 95-F8BT and pure F8BT, while an increase is experimentally observed. These results clearly indicate that the ASE properties of the investigated blends are not determined by the variations of the wave-guiding properties of the various samples. Moreover we rule out, too, any possible film thickness variation in order to explain the red-shift of the stimulated emission band detected between 540 and 570 nm (see Fig. 2). There is no such a thickness variation among the samples. Such a red-shift (about 30 nm) can not be simply explained by taking into account the red-shift of the PL peak: indeed the PLs shift only of about 15 nm (see Fig. S2 in the S.I.). The ASE red-shift can be explained by a combination of the PLs red-shift due to the increasing acceptor concentration and a variation in the self-absorption by the blend [45].

Time Resolved Photoluminescence. We then investigated the F8BT relaxation dynamics (see Figg. 3 and 4) collected at 530 nm. The F8BT PL shows a quasi-monoexponential decay with a lifetime of about 1.4 ns for F8BT content up to 50%, followed by a progressive decrease for higher F8BT content, down to 0.76 ns in pure F8BT (see the lifetime plot in Fig. 3).

The increased FRET efficiency with acceptor loading should be linked with an increase of the acceptor luminescence lifetime. On the contrary our data (see Fig. 3 and 4) clearly show that, increasing the acceptor content, the luminescence lifetime decreases. This behavior is likely due to the activation and the progressive increase of intermolecular energy migration within the
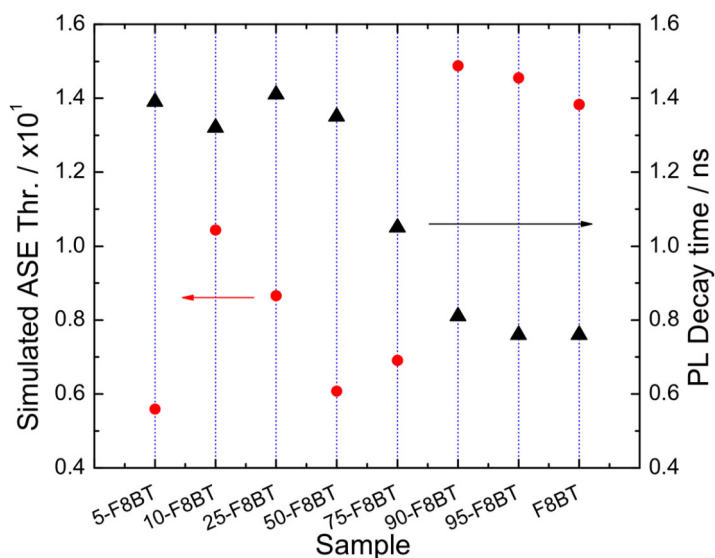
11

Figure 3: Simulated ASE threshold (circular red) and PL decay time (triangular black) of the analyzed X-F8BT samples.

F8BT phase towards quenching sites [46].

In order to separate the FRET and the aggregation contribution in the F8BT relaxation dynamics, we also realized control samples by blending the F8BT with an inert polymer, namely Poly(methyl methacrylate) (PMMA). A progressive decrease of the PL decay time as the F8BT content increases is still observed (see Fig. S3 in the S. I.), confirming the attribution of the F8BT lifetime reduction in the active blends to a progressive increase of the intermolecular energy migration towards quenching sites. Our results evidences that F8BT intermolecular energy migration becomes important for F8BT content above 50%, and should then decrease the ASE in this content range. This is clearly not consistent with the disappearance of ASE already for 25% of F8BT, and with the presence of ASE for F8BT contents above

12
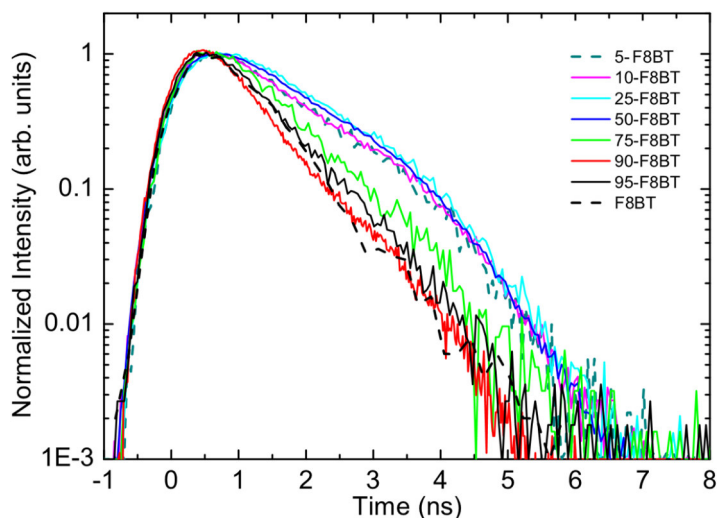
Figure 4: F8BT relaxation dynamics in all the investigated samples.

90%. On the contrary the ASE threshold increase from 90% of F8BT to pure F8BT is qualitatively consistent with the increase of F8BT aggregation.

In these samples most of the pump laser is directly absorbed by F8BT (see Tab. S1 in the S. I.), thus the ASE properties are likely related to the F8BT emission efficiency and to the wave-guiding efficiency of the film (see Fig. S4 and S5 in the S. I. and relative comments).

With the purpose of finding a possible explanation for our results, we have performed a morphological characterization by Laser Scanning Microscopy of all of the samples.

Blends Morphology. Fig. 5 reports the $7.5 \times 7.5 \mu m^2$ F8BT PL maps of the samples recorded at 605 ± 30 nm, along with their 2D Fast Fourier Transform (2D FFT) in the insets (i) to g)). It is possible to list the following main considerations:
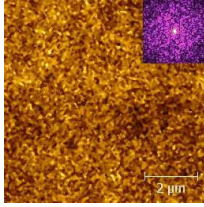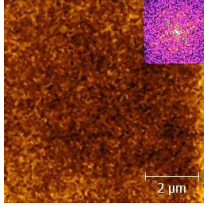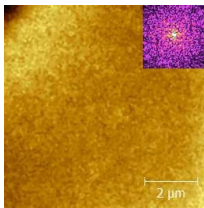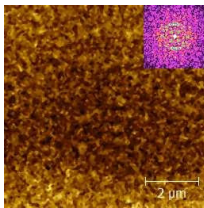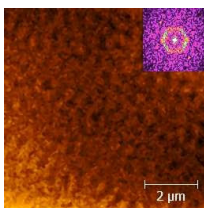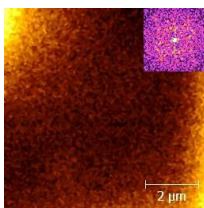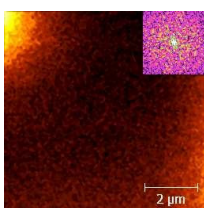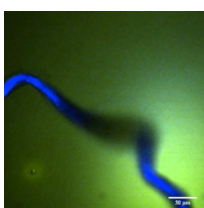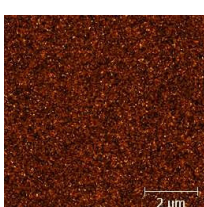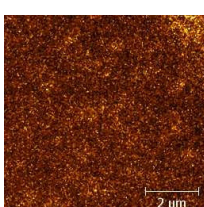
a) 5-F8BT

b) 10-F8BT

c) 25-F8BT

d) 50-F8BT

e) 75-F8BT

f) 90-F8BT

g) 95-F8BT

h) 25-F8BT dual channel

i) 50-F8BT, PF8 channel

j) 75-F8BT, PF8 channel

Figure 5: 2D PL maps of the PF8:F8BT samples: a) 5-F8BT, b) 10-F8BT, c) 25-F8BT,[14] d) 50-F8BT, e) 75-F8BT, f) 90-F8BT, g) 95-F8BT, h) 25-F8BT dual channel map, i) 50-F8BT and j) 75-F8BT. Maps from a) to g) have been collected at the F8BT emission channel, 7.5×7.5 μm^2, pump at 488 nm. Map h) has been collected at both PF8 (blue) and F8BT (green) emission channels, $212 \times 212 \mu$m^2, pump at 405 nm. Maps i) and j) have been collected at the PF8 emission channel, 7.5×7.5 μm^2, pump at 405 nm.

- All the samples showing ASE (a), b), f) and g)) are morphologically homogeneous (in both the collection channels: the 450 nm collection channel images, measured by pumping with the 405 nm laser source, are reported in the S.I, Fig. S6). This observation is confirmed by the absence of any particular features in their 2D FFT.

- the 25-F8BT sample is characterized by a macroscopic phase segregation between the two polymers (see h) in Fig. 5), in particular the PF8 mainly aggregates in elongated structures (that are evenly distributed all over the sample: several sample regions have been checked, all showing such structures), while the F8BT appears to be uniform among the PF8 structure. The origin of this sample structure is actually unclear, but this does not influence the general conclusions of this work: the presence of these structures may add an optical loss channel due to scattering.

- in the 50-F8BT and in the 75-F8BT samples the F8BT tends to segregate in honeycomb-like structure, evidenced by the features appearing in the 2D FFT). These features have dimension of about 480 nm and 550 nm respectively, as calculated from the 2D FFT. This pattern is visible in the F8BT emission channel only, while the PF8 emission channel shows a more homogeneous pattern in the 50-F8BT and the 75-F8BT samples (i) and j) in Fig. 5). The PF8 phase is evenly dispersed in the blend volume (see i) and j) in Fig. 5). This means that

15

energy transfer mechanism is still efficient [42], but the overall patterned structure may increase the optical losses, preventing the ASE to occur from the blends [47]

Thus it is clear how the ASE is suppressed in the less uniform and less homogeneous samples, irrespective of the efficient energy transfer mechanism between the donor polymer and the acceptor polymer. The donor-to-acceptor concentration ratio should then be carefully optimized in the particular blend system searching for a good compromise between low ASE threshold and optimal overall blend morphology. Moreover, it has been recently demonstrated that polymer morphology has a negligible impact on the optical gain properties of organic waveguide based on single polymer active layer [48, 49], questioning the importance of the sample morphology for ASE to occur. Our results clearly demonstrate that this is not true in the case of active layers composed of *blends* of PF8:F8BT. Indeed the overall sample morphology has a direct impact on the optical gain properties of the organic waveguide.

4. Conclusions

In conclusion we have shown that the ASE threshold behavior as a function of donor-to-acceptor ratio in PF8:F8BT blends is strictly correlated on the blend morphology rather than on just the concentration ratio and/or the FRET efficiency between the PF8 donor and the F8BT acceptor. Phase segregation of one of the species prevents the stimulated emission process even in presence of a very efficient energy transfer mechanism. This is reasonably due to increased optical losses inside the polymeric waveguide. Thus, since phase segregation is a typical property of polymeric blends, we can infer that our results can be generalized to other polymeric host-guest

systems, showing that even if the optoelectronic properties of the two species are the best one for an energy transfer mechanism to occur, the blend morphology can substantially vary as a function of the relative concentration, directly affecting the blend optical gain properties.

Although the reported ASE thresholds are not among the lower as reported so far in the literature, the selected system is important since it is a typical prototype provided with the good energetics for a FRET to occur, with the purpose of demonstrating how the morphological phase separation properties of a blend can influence the optical gain properties of a "good" blend (from the energetic point of view), up to completely suppress any optical gain.

5. Acknowledgments

6. References

[1] H. Shirakawa, E. J. Louis, A. G. MacDiarmid, C. K. Chiang, A. J. Heeger, J. Chem. Soc. Chem. Commun. (1977) 578–

580`doi:10.1039/C39770000578`.

[2] Organic electronics for a better tomorrow: (2012).

URL `http://www.rsc.org/globalassets/`

```
04-campaigning-outreach/realising-potential-of-scientists/
research-policy/global-challenges/organic-electronics-for-a-
better-tomorrow1.pdf
```

[3] E. Moons, J. Phys. Condens. Matter 14 (47) (2002) 12235.

[4] B. Imre, B. Puknszky, Eur. Pol. J. 49 (2013) 1215 – 1233.

[5] Y.-C. Hung, C.-H. Su, H.-W. Huang, J. App. Phys. 111 (2012) 113107.

[6] J. Mysliwiec, L. Sznitko, S. Bartkiewicz, A. Miniewicz, Z. Essaidi, F. Kajzar, B. Sahraoui, Appl. Phys. Lett. 94 (2009) 241106.

[7] J. F. Galisteo-L´opez, M. Ibisate, C. L´opez, J. Phys. Chem. C 118 (2014) 9665–9669.

[8] M. Anni, S. Lattante, J. Phys. Chem. C 119 (2015) 21620–21625.

[9] X. Yang, J. Loos, Macromolecules 40 (2007) 1353–1362.

[10] Y. Shi, J. Liu, Y. Yang, Journal of Applied Physics 87 (2000) 4254–4263.

[11] M. Shtein, J. Mapel, J. B. Benziger, S. R. Forrest, Appl. Phys. Lett. 81 (2002) 268–270.

[12] X.-J. She, C.-H. Liu, Q.-J. Sun, X. Gao, S.-D. Wang, Org. Electronics 13 (2012) 1908 – 1915.

[13] M. Anni, S. Lattante, R. Cingolani, G. Gigli, G. Barbarella, L. Favaretto, Applied Physics Letters 83 (2003) 2754–2756.

[14] J. Y. Kim, S. H. Park, K. Lee, I. S. Yum, S. H. Jin, Appl. Phys. Lett. 81 (2002) 1732–1734.

[15] J. Du, E. Xu, H. Zhong, F. Yu, C. Liu, H. Wu, D. Zeng, S. Ren, J. Sun,

Y. Liu, A. Cao, Q. Fang, J. Polym. Sci. A Polym. Chem. 46 (2008) 13761387.

[16] Z. E. Lampert, J. M. Papanikolas, C. Lewis Reynolds, Appl. Phys. Lett. 102 (2013) 073303.

[17] J. Li, F. Laquai, G. Wegner, Chem. Phys. Lett. 478 (1-3) (2009) 37–41.

[18] G. Tsiminis, Y. Wang, P. Shaw, A. Kanibolotsky, I. Perepichka, M. Dawson, P. Skabara, G. Turnbull, I. Samuel, Appl. Phys. Lett. 94 (2009) 243304.

[19] D. Schneider, T. Rabe, T. Riedl, T. Dobbertin, O. Werner, M. Kr̈ager, E. Becker, H.-H. Johannes, W. Kowalsky, T. Weimann, J. Wang, P. Hinze, A. Gerhard, P. Sẗassel, H. Vestweber, Appl. Phys. Lett. 84 (2004) 4693.

[20] S. Lattante, M. Anni, M. Salerno, L. Lagonigro, R. Cingolani, G. Gigli, M. Pasini, S. Destri, W. Porzio, Opt. Mater. 28 (2006) 1072.

[21] T. Virgili, J. Clark, J. Cabanillas-Gonzalez, L. Bazzana, K. C. Vishnubhatla, R. Osellame, R. Ramponi, G. Lanzani, J. Mater. Chem. 20 (2010) 519–523.

[22] M. Anni, S. Lattante, ISRN Materials Science doi:http://dx.doi.org/10.1155/2014/856716.

[23] M. Anni, R. Rella, J. Phys. Chem. B 114 (2010) 1559–1561.

[24] M. D. McGehee, A. J. Heeger, Adv. Mater. 12 (2000) 1655 – 1668.

[25] S. Z. Bisri, T. Takenobu, Y. Iwasa, J. Mater. Chem. C 2 (2014) 2827– 2836.

[26] S. Klinkhammer, X. Liu, K. Huska, Y. Shen, S. Vanderheiden, S. Valouch, C. Vannahme, S. Br̈ase, T. Mappes, U. Lemmer, Opt. Express 20 (2012) 6357–6364.

[27] F. Hide, M. A. D´ıaz-Garca, B. J. Schwartz, M. R. Andersson, Q. Pei, A. J. Heeger, Science 273 (1996) 1833.

[28] R. H. Friend, G. J. Denton, N. Tessler, M. A. Stevens, Adv. Mater. 9 (1997) 547.

[29] M. D. McGehee, R. Gupta, S. Veenstra, E. K. Miller, M. A. Diaz-Garcia, A. J. Heeger, Phys. Rev. B 58 (1998) 7035–7039.

[30] A. K. Sheridan, A. R. Buckley, A. M. Fox, A. Bacher, D. D. C. Bradley, I. D. W. Samuel, J. Appl. Phys. 92 (2002) 6367–6371.

[31] R. Gupta, M. Stevenson, A. Dogariu, M. D. McGehee, J. Y. Park, V. Srdanov, A. J. Heeger, H. Wang, Appl. Phys. Lett. 73 (24) (1998) 3492– 3494.

[32] M. Anni, E. Alemanno, A. Cret´ı, C. Ingrosso, A. Panniello, M. Striccoli, M. L. Curri, M. Lomascolo, J. Phys. Chem. A 114 (2010) 2086–2090.

[33] A. Camposeo, E. Mele, L. Persano, D. Pisignano, R. Cingolani, Phys. Rev. B 73 (2006) 165201.

[34] R. Xia, P. N. Stavrinou, D. D. C. Bradley, Y. Kim, J. Appl. Phys. 111 (12) (2012) 123107.

[35] C. Pan, K. Sugiyasu, M. Takeuchi, Chem. Commun. 50 (2014) 11814– 11817.

[36] A. Buckley, M. Rahn, J. Hill, J. Cabanillas-Gonzalez, A. Fox, D. Bradley, Chem. Phys. Lett. 339 (2001) 331 – 336.

[37] C. I. Wilkinson, D. G. Lidzey, L. C. Palilis, R. B. Fletcher, S. J. Martin, X. H. Wang, D. D. C. Bradley, Appl. Phys. Lett. 79 (2001) 171–173.

[38] M. Ariu, M. Sims, M. D. Rahn, J. Hill, A. M. Fox, D. G. Lidzey, M. Oda, J. Cabanillas-Gonzalez, D. D. C. Bradley, Phys. Rev. B 67 (2003) 195333.

[39] A. Perevedentsev, S. Aksel, K. Feldman, P. Smith, P. N. Stavrinou, D. D. C. Bradley, J. Polym. Sci. Pol. Phys. 53 (1) (2015) 22–38.

[40] L. Sznitko, J. Mysliwiec, A. Miniewicz, Journal of Polymer Science Part B: Polymer Physics 53 (2015) 951–974.

[41] X. Wu, W. Fang, A. Yamilov, A. A. Chabanov, A. A. Asatryan, L. C. Botten, H. Cao, Phys. Rev. A 74 (2006) 053812.

[42] J. Hill, S. Y. Heriot, O. Worsfold, T. H. Richardson, A. M. Fox, D. D. C. Bradley, Phys. Rev. B 69 (2004) 041303.

[43] M. Anni, A. Perulli, G. Monti, J. Appl. Phys. 111 (2012) 093109.

[44] M. Campoy-Quiles, G. Heliotis, R. Xia, M. Ariu, M. Pintani, P. Etchegoin, D. C. Bradley, Adv. Funct. Mater. 15 (6) (2005) 925–933.

[45] E. M. Calzado, P. G. Boj, M. A. D′ıaz-Garc′ıa, Int. J. Mol. Sci. 11(6) (2010) 2546.

[46] L. M. Herz, C. Silva, A. C. Grimsdale, K. Mu¨llen, R. T. Phillips, Phys. Rev. B 70 (2004) 165207.

[47] I. B. Martini, I. M. Craig, W. C. Molenkamp, H. Miyata, S. H. Tolbert, B. J. Schwartz, Nat. Nanotechnol. 2 (2007) 647 – 652.

[48] Z. E. Lampert, C. L. Reynolds, J. M. Papanikolas, M. O. Aboelfotoh, J. Phys. Chem. B 116 (2012) 12835–12841.

[49] Z. E. Lampert, S. E. Lappi, J. M. Papanikolas, C. Lewis Reynolds, M. Osama Aboelfotoh, J. Appl. Phys. 113 (23) (2013) 233509.